REGULAR ARTICLE

Calculation of dispersion interactions with the geminal-based ring Coupled Cluster Doubles method

Á. Margócsy[1,2] · Á. Szabados[2]

Abstract

The performance of the recently developed multi-reference extension of ring coupled cluster doubles is investigated for dispersion energy calculations, applied to the generalized valence bond wave function. The leading-order contribution to the dispersion energy is shown to have the correct asymptotic behaviour. Illustrative calculations on noble gas dimers are presented.

Keywords Coupled Cluster Doubles · Ring approximation · Dispersion interaction · Generalized valence bond · Cumulants

1 Introduction

Calculation of dispersion energy between atoms or molecules is a long-standing problem of quantum chemistry. Physically, dispersion interaction arises from the charge density fluctuations of the subsystems, leading to weakly bound states between, for example, closed-shell partners even if they lack permanent electric moments. The importance of dispersion interaction in both chemical and biological systems cannot be overemphasized.

For two subsystems at a large separation distance R, the asymptotic dispersion energy is manifested as [1]

$$E_{\text{disp.}} \approx -\frac{C_6}{R^6}, \tag{1}$$

✉ Á. Szabados
   szabados@caesar.elte.hu

   Á. Margócsy
   margocsy@coulson.chem.elte.hu

1 Doctoral School of Chemistry, Faculty of Science, ELTE Eötvös Loránd University, POB 32, Budapest 1518, Hungary

2 Laboratory of Theoretical Chemistry, Institute of Chemistry, Faculty of Science, ELTE Eötvös Loránd University, POB 32, Budapest 1518, Hungary

provided that R is not large enough for retardation effects to become noticeable. The dispersion coefficient C_6 can be expressed in terms of the frequency-dependent polarizability (FDP) of each subsystem. Providing an equally accurate description of dispersion both in the equilibrium and in the asymptotic regime has remained a challenge for electronic structure methods to this day.

Mean-field methods, such as Hartree–Fock (HF), cannot even qualitatively account for dispersion; such phenomena are usually introduced via correlation corrections, obtained, for example by perturbation theory (PT). Szabo and Ostlund showed [2] that a supermolecular Møller–Plesset PT2 (MP2) calculation gives rise to dispersion energy exhibiting the correct asymptotic behaviour [i.e. conforming (1)], but with C_6 calculated only at the level of uncoupled HF [3]. An alternative of the supermolecule approach is the symmetry-adapted perturbation theory (SAPT) of Jeziorski et al. (see Ref. [4] and references cited therein), in which the intersystem interaction is treated as perturbation. The relationship between supermolecular MP and SAPT has been investigated in detail [5].

The quality of the supermolecular approach can be improved by applying corrections more involved than MP2, e.g. the all-order inclusion of direct ring-type Goldstone diagrams (and possibly certain kinds of exchange ring diagrams) [6]. In the random phase approximation (RPA), the effect of these diagrams can be easily taken into account. Different variants of RPA (distinguished by the different degrees of including exchange diagrams) improve quantitatively on the MP2

results, but not all of them lead to a correct expression for the dispersion coefficient [2, 7].

Another way to include higher-order diagrams in the energy is through coupled cluster (CC) [8, 9]. The CC method with single, double and perturbative triple excitations (CCSD(T)) [10] yields essentially exact results for intermolecular interactions and is often used as benchmark in such cases. The CC model also provides a way to sum up only ring diagrams. The ring CCD (rCCD) approach, originally introduced by Čížek [11], is a computationally less demanding alternative to CCSD(T), scaling as $\mathcal{O}(n^6)$ (in some cases $\mathcal{O}(n^5)$ [12]) instead of $\mathcal{O}(n^7)$ (n being the number of basis functions). The formal equivalence of certain kinds of RPA and rCCD methods has been noticed by many [6, 11–13].

RPA and rCCD have recently seen a renewed interest in the context of density functional theory [14–16], since correlation energy functionals derived from RPA can serve to construct post-Kohn–Sham models [17] and can account for dispersion effects. Development of new methods (e.g. RPA+SOSEX [18, 19] or renormalized PT2 [20]) and refinement of existing ones (e.g. inclusion of explicitly correlated terms in rCCD [21]) have been reported. The combination of range-separated hybrid functionals with RPA/rCCD has also proved to be a successful method for calculating dispersion energy [22, 23].

Dispersion interaction is a result of the dynamic (weak) part of electron correlation. It is still interesting to investigate the performance of multi-reference (MR) methods (developed to give reasonable results for strongly correlated systems) when it comes to calculating weak interactions. This is the purpose of the present study.

MR methods assume a multi-determinantal reference function. The reference function we are concerned with in this work is the antisymmetrized product of strongly orthogonal geminals (APSG) [24]. The APSG wave function for an N-electron singlet system (N being even) is constructed using two-electron functions (geminals) with a handful of orbitals assigned to each of them. The strong orthogonality condition implies the mutually disjoint distribution of orbitals among the geminals [25]. The wave function takes a product form:

$$|\text{APSG}\rangle = \prod_{\mathcal{P}=1}^{N/2} \psi_{\mathcal{P}}^{\dagger}|\text{vac}\rangle,$$

with

$$\psi_{\mathcal{P}}^{\dagger} = \sum_{p \in \mathcal{P}} c_p a_{p\alpha}^{\dagger} a_{p\beta}^{\dagger}.$$

Here, $|\text{vac}\rangle$ is the true vacuum, $a_{p\sigma}^{\dagger}$ is the creation operator of spatial orbital ϕ_p with spin σ and $\mathcal{P}$ is the index of the geminal ϕ_p belongs to. We arrive at a particularly simple wave function if each geminal consists of at most two orbitals; this choice defines the generalized valence bond (GVB) method

[26]. We work on the basis of natural orbitals diagonalizing the one-particle reduced density matrix. The geminal coefficients obey the relation $|c_p|^2 = n_p$, where $n_p \in [0, 1]$ is the occupation number. For later use, we also introduce the hole occupation number $\bar{n}_p = 1 - n_p$. During an APSG calculation, geminal coefficients and orbitals are optimized simultaneously. The intrageminal part of electron correlation is taken into account, while the intergeminal interaction is treated in a mean-field manner. While APSG usually provides a good starting point for the description of left–right correlation, it is no better at calculating dispersion energy than HF. Various correction schemes applied to APSG can, however, tackle this problem. The APSG-based linearized CC of Zoboki et al. was shown to give very accurate results for a He dimer [27]. The extended RPA for APSG (APSG-ERPA) developed by Pernal et al. [28, 29] was also shown to account for a great portion of dispersion energy; later this approach was further refined by electron-groups embedding [30, 31].

We presented our approach to GVB-based correction methods in Ref. [32]: an MR extension of rCCD, formulated in the internally contracted (ic) MR-CC framework of Mukherjee et al. [33]. The method greatly improves on GVB results in various scenarios (bond breaking, conformational barriers, etc.) and gives results somewhat similar to ERPA, although the formal RPA-rCCD correspondence does not hold anymore [34]. In this paper, we assess GVB-rCCD on the example of calculating interaction energy between noble gas atoms.

The rest of the paper is organized as follows: in Sect. 2, we demonstrate that in leading order the spin-orbital GVB-rCCD energy shows the correct asymptotics, according to (1), and argue that the full rCCD energy correction shows a similar decay. In Sect. 3, a brief review of spin-free GVB-rCCD is given, and numerical results are presented for the interaction energy of He_2 and Ne_2. Conclusions are drawn in Sect. 4.

Atomic units are used throughout the paper.

2 Asymptotic behaviour of GVB-rCCD

Our ic-MR-CC formalism is based on the MR extension of the generalized normal ordering (denoted by ::) and the corresponding generalized Wick theorem (MR-GWT) of Kutzelnigg and Mukherjee [35]. The correlated ground-state wave function is parametrized by a normal-ordered exponential wave operator, originally proposed by Lindgren [36]:

$$|\Psi\rangle =: \exp(T) : |\Phi\rangle, \tag{2}$$

where $|\Phi\rangle$ can be—in principle—any MR wave function, and

$$T = \frac{1}{4} \sum_{\substack{I,A \\ J,B}} t_{AB}^{IJ} a_{IJ}^{AB},$$

with $a_{IJ}^{AB} = a_A^\dagger a_B^\dagger a_J a_I$. Indices I, J, K, L and A, B, C, D correspond to arbitrary core/active and active/virtual spin orbitals, respectively (excluding a few ill-defined cases; see Sect. 3). The working equations are obtained by plugging (2) in the Schrödinger equation and projecting with $\langle \Phi |$, and $\langle \Phi | : a_{AB}^{IJ} :$. The resulting formulae are to be evaluated using the MR-GWT, leading to an expansion in terms of density cumulants. Due to the incredibly large number of terms generated by the MR-GWT, it is virtually impossible to proceed without further approximations. A way of arriving at a manageable set of equations is given by the MR extension of the ring approximation. Following the same procedure as in Ref. [32], one arrives at the spin-orbital variant of the MR-rCCD equations:

$$\Delta E = \frac{1}{4} \sum_{\substack{I,A \\ J,B}} V_{IJ}^{AB} t_{AB}^{IJ} n_I n_J \bar{n}^A \bar{n}^B, \tag{3}$$

$$0 = V_{AB}^{IJ} - \sum_K \mathcal{A}^{IJ} \left(F_K^J t_{AB}^{IK} \right) n_K + \sum_C \mathcal{A}_{AB} \left(F_B^C t_{AC}^{IJ} \right) \bar{n}^C$$
$$+ \sum_{K,C} \left(V_{AK}^{IC} t_{CB}^{KJ} + V_{BK}^{JC} t_{CA}^{KI} \right) n_K \bar{n}^C$$
$$+ \sum_{\substack{K,C \\ L,D}} t_{AC}^{IK} V_{KL}^{CD} t_{DA}^{LJ} n_K n_L \bar{n}^C \bar{n}^D, \tag{4}$$

where $\mathcal{A}^{IJ} = I - P^{IJ}$ is the antisymmetrizing operator. The MR-rCCD equations (3) and (4) formally look just like their single-reference (SR) counterparts, but contain "dressed" one- and two-particle vertices F and V instead of "bare" vertices f (the Fockian) and $\tilde{v}$ (the antisymmetrized two-electron integral). The explicit form of these vertices is given in "Appendix 1". The dressed vertices are functions of density cumulants and therefore contain a zeroth-order description of static electron correlation ($|\Phi\rangle$ being MR). If $|\Phi\rangle$ happens to be a single Slater determinant, then all cumulants vanish, the dressed vertices fall back to bare ones, and the usual SR-rCCD formulae are retrieved. Setting $|\Phi\rangle = |GVB\rangle$ defines GVB-rCCD.

Using the SR-like energy denominator

$$\epsilon_I^A = \bar{n}^A F_A^A - n_I F_I^I \tag{5}$$

to solve (4) iteratively and plugging back the iterations into (3) leads to a PT-like expansion for the energy correction:

$$\Delta E = -\frac{1}{4} \sum_{\substack{I,A \\ J,B}} \frac{V_{IJ}^{AB} V_{AB}^{IJ}}{\epsilon_I^A + \epsilon_J^B} n_I \bar{n}^A n_J \bar{n}^B + \cdots \tag{6}$$

Because of its formal similarity to a second-order PT energy, we shall refer to the first term on the rhs of (6) as $E^{(2)}$. The connectedness of the formulae and the vertices ensures the extensivity of the method, provided that intersystem cumulants vanish (which is always the case for closed-shell subsystems [37]).

The spin-orbital SR-rCCD energy correction is known to be somewhat "incomplete": in its diagrammatic expansion, ring-type antisymmetrized Goldstone diagrams beyond second order contain an extra factor of 1/2. This factor would be cancelled by the crossed-ring terms (with, for example, amplitudes t_{CB}^{IK}) missing in rCCD. An easy way to make the diagrams complete (without double counting $E^{(2)}$) is through the modified energy formula [6, 38] $\Delta \tilde{E} = 2\Delta E - E^{(2)}$. The same reasoning applies to our spin-orbital MR-rCCD energy; however, we shall not pursue this question any further.

Most RPA/rCCD-like methods do not give a satisfactory description of long-range dispersion interactions [2, 23]: while they produce the correct $\sim 1/R^6$ decay, the dispersion coefficient C_6 can rarely be expressed in terms of FDPs. We show here that the leading-order contribution of the GVB-rCCD energy exhibits the correct asymptotics and its dispersion coefficient can be expressed in terms of FDP-like quantities. We believe that this result gives valuable insight into how cancellations occur in the dressed vertices. We also argue that the $\sim 1/R^6$ decay holds for the complete GVB-rCCD energy as well, but without the correct form of C_6. The derivation follows closely the MP2 analysis of Szabo and Ostlund [2, 7] and can be thought of as a possible MR extension.

We start from $E^{(2)}$, the leading-order energy in (6), and consider singlet systems. After breaking up the spin-orbital indices to a spatial and a spin part (e.g. $A = a\sigma$), and using relations $n_i := n_{i\alpha} = n_{i\beta}$ and (27), one finds that the energy denominator is spin-independent: $\epsilon_i^a := \epsilon_{i\alpha}^{a\alpha} = \epsilon_{i\beta}^{a\beta}$. The summation over the remaining spin degrees of freedom can be then easily performed with the help of (28). Utilizing the spin-free two-particle vertex $\mathcal{V}_{ij}^{ab}$ (given in "Appendix 1"), $E^{(2)}$ takes the form:

$$E^{(2)} = -\frac{1}{12} \sum_{i,j,a,b} \frac{\mathcal{V}_{ij}^{ab} \left(2\mathcal{V}_{ab}^{ij} + \mathcal{V}_{ba}^{ij} \right)}{\epsilon_i^a + \epsilon_j^b} n_i \bar{n}^a n_j \bar{n}^b. \tag{7}$$

We now consider a supersystem composed of two closed shell, electrically neutral atoms $\mathbb{A}$ and $\mathbb{B}$ separated at a large distance R. Orbitals are assumed to be localized on either $\mathbb{A}$ or $\mathbb{B}$. Based on this, indices in (7) can be categorized, resulting in two intrasystem terms ($i, j, a, b \in \mathbb{A}$ or $i, j, a, b \in \mathbb{B}$) and the remaining intersystem term:

$$E^{(2)} = E_{\mathbb{A}}^{(2)} + E_{\mathbb{B}}^{(2)} + E_{disp}^{(2)}.$$

Turning to the dispersion energy, the differential overlap of the subsystems is exponentially small, making most of the

intersystem integrals negligible. Intersystem cumulants also vanish due to the strongly orthogonal geminals being localized on subsystems. Therefore, cases like $(i, j \in \mathbb{A}; a, b \in \mathbb{B})$ or $(i, j, a \in \mathbb{A}; b \in \mathbb{B})$ can be safely neglected. The only remaining cases are of the form

$$(i, a \in \mathbb{A}; j, b \in \mathbb{B}) \rightarrow \mathcal{V}_{ij}^{ab} \approx 4W_{ij}^{ab}, \tag{8}$$

$$(j, a \in \mathbb{A}; i, b \in \mathbb{B}) \rightarrow \mathcal{V}_{ij}^{ab} \approx -2W_{ji}^{ab}. \tag{9}$$

The expression of vertex W_{ij}^{ab} is given as

$$W_{ij}^{ab} = v_{ij}^{ab} + \frac{1}{2} \sum_{p,q} \left(\frac{1}{n_i \bar{n}^a} v_{jp}^{bq} \Lambda_{iq}^{ap} + \frac{1}{n_j \bar{n}^b} v_{ip}^{aq} \Lambda_{jq}^{bp} \right)$$
$$+ \frac{1}{4} \frac{1}{n_i \bar{n}^a n_j \bar{n}^b} \sum_{p,q,r,s} v_{pr}^{qs} \Lambda_{iq}^{ap} \Lambda_{js}^{br} \tag{10}$$
$$= \int d^3 r_1 \int d^3 r_2 \frac{\Omega_i^a(\mathbf{r}_1)\Omega_j^b(\mathbf{r}_2)}{|\mathbf{r}_1 - \mathbf{r}_2|},$$

and

$$\Omega_i^a(\mathbf{r}) = \phi_i^*(\mathbf{r})\phi_a(\mathbf{r}) + \frac{1}{2n_i \bar{n}^a} \sum_{p,q} \Lambda_{iq}^{ap} \phi_p^*(\mathbf{r})\phi_q(\mathbf{r}).$$

Using the partial trace relation [39, 40]

$$\sum_p \Lambda_{ip}^{ap} = -2\delta_i^a n_i \bar{n}^a,$$

it is easy to see that $\Omega_i^a(\mathbf{r})$ integrates to zero for all i, a:

$$\int d^3 r \, \Omega_i^a(\mathbf{r}) = \delta_i^a + \frac{1}{2n_i \bar{n}^a} \sum_p \Lambda_{ip}^{ap} = 0. \tag{11}$$

Quantities W_{ab}^{ij}, $\Omega_a^i(\mathbf{r})$ appearing in the asymptotic limit of $\mathcal{V}_{ab}^{ij}$ can be obtained analogously to the above. Based on "Appendix 1", the relation of $\mathcal{V}_{ab}^{ij}$ and $\mathcal{V}_{ij}^{ab}$ is Hermitian conjugation, and the same holds for W_{ab}^{ij} and $\Omega_a^i(\mathbf{r})$.

Substituting (8), (9) and their Hermitian conjugate into (7) gives

$$E_{disp}^{(2)} \approx -4 \sum_{\substack{i,a \in \mathbb{A} \\ j,b \in \mathbb{B}}} \frac{W_{ij}^{ab} W_{ab}^{ij}}{\epsilon_i^a + \epsilon_j^b} n_i \bar{n}^a n_j \bar{n}^b. \tag{12}$$

We shall now make use of the multipole expansion of the Coulomb potential:

$$\frac{1}{|\mathbf{r}_1 - \mathbf{r}_2|} = \frac{1}{|\mathbf{r} - \mathbf{R}|} = \frac{1}{R} + \frac{\mathbf{n} \cdot \mathbf{r}}{R^2} + \frac{3(\mathbf{n} \cdot \mathbf{r})^2 - r^2}{2R^3} + \mathcal{O}(R^{-4}), \tag{13}$$

with $\mathbf{n}$ being a unit vector parallel to $\mathbf{R} = \mathbf{R}_{\mathbb{B}} - \mathbf{R}_{\mathbb{A}}$ and $\mathbf{r} = \mathbf{r}_{\mathbb{A}1} - \mathbf{r}_{\mathbb{B}2}$ being the difference of electronic coordinates measured from the nuclei.

Inserting (13) into (10), the appearance of anomalous terms proportional to $1/R$ or $1/R^2$ in W_{ij}^{ab} is prevented by (11). Keeping only the first non-vanishing term yields

$$W_{ij}^{ab} \approx \frac{1}{R^3} \boldsymbol{\mu}_i^a \boldsymbol{\tau} \boldsymbol{\mu}_j^b, \tag{14}$$

where $\boldsymbol{\tau} = \mathbf{I} - 3\mathbf{n} \otimes \mathbf{n}$ is a symmetric matrix ($\otimes$ being the dyadic product of the 3-vectors) and $\boldsymbol{\mu}_i^a$ can be interpreted as the transition dipole moment with a cumulant correction:

$$\boldsymbol{\mu}_i^a = - \int d^3 r' \, \Omega_i^a(\mathbf{r}')\mathbf{r}' = \frac{1}{2n_i \bar{n}^a} \langle \text{GVB} | \boldsymbol{\mu} : E_i^a : | \text{GVB} \rangle. \tag{15}$$

In the above, $E_i^a = a_{i\alpha}^{a\alpha} + a_{i\beta}^{a\beta}$ is a spin-free excitation operator. As before, the cumulant-corrected transition dipole $\boldsymbol{\mu}_b^j$ is the Hermitian conjugate of $\boldsymbol{\mu}_j^b$.

Substituting (14) and its Hermitian conjugate into (12), we have $E_{\text{disp}}^{(2)} \approx -C_6/R^6$, with the coefficient C_6 given by

$$C_6 = 4 \sum_{\substack{i,a \in \mathbb{A} \\ j,b \in \mathbb{B}}} \frac{n_i \bar{n}^a n_j \bar{n}^b}{\epsilon_i^a + \epsilon_j^b} (\boldsymbol{\mu}_i^a \boldsymbol{\tau} \boldsymbol{\mu}_j^b)(\boldsymbol{\mu}_a^i \boldsymbol{\tau} \boldsymbol{\mu}_b^j).$$

Assuming the positivity of ϵ_i^a (as argued in "Appendix 3"), we can use the identity

$$\frac{1}{\epsilon + \epsilon'} = \frac{2}{\pi} \int_0^\infty d\omega \frac{\epsilon \epsilon'}{(\epsilon^2 + \omega^2)(\epsilon'^2 + \omega^2)} \quad (\epsilon, \epsilon' > 0),$$

to obtain the final form of C_6, reading as

$$C_6 = \int_0^\infty \frac{d\omega}{2\pi} \text{Tr} \big[\boldsymbol{\alpha}_{\mathbb{A}}(i\omega)\boldsymbol{\tau} \boldsymbol{\alpha}_{\mathbb{B}}(i\omega)\boldsymbol{\tau} \big], \tag{16}$$

where orbitals were taken to be real for simplicity, and we introduced the FDP-like quantities:

$$\boldsymbol{\alpha}_{\mathbb{A}}(i\omega) = 4 \sum_{i,a \in \mathbb{A}} \frac{\epsilon_i^a n_i \bar{n}^a}{(\epsilon_i^a)^2 - (i\omega)^2} \boldsymbol{\mu}_i^a \otimes \boldsymbol{\mu}_a^i.$$

For isotropic subsystems, $\boldsymbol{\alpha}_{\mathbb{A}}(i\omega)$ must be proportional to the unit tensor: $\boldsymbol{\alpha}_{\mathbb{A}}(i\omega) = \alpha_{\mathbb{A}}(i\omega)\mathbf{I}$. Using this together with $\text{Tr}[\boldsymbol{\tau}^2] = 6$ allows us to write (16) as

$$C_6 = \frac{3}{\pi} \int_0^\infty d\omega \, \alpha_{\mathbb{A}}(i\omega)\alpha_{\mathbb{B}}(i\omega).$$

The obtained expressions are formally similar to the PT-based formulae of Szabo and Ostlund [2], but involve cumulant-dependent quantities, such as $\boldsymbol{\mu}_i^a$ or $\boldsymbol{\alpha}_{\mathbb{A}}(i\omega)$.

As it was demonstrated in this section, dressed vertices show the proper asymptotic behaviour, just like their

bare counterparts. Based on this, one could continue the analysis and investigate the asymptotics of the full rCCD equations (3) and (4); while the $\sim 1/R^6$ decay could be argued this way, the coefficient C_6 would not exhibit the form of (16) involving FDPs.

3 Numerical results for noble gas dimers in spin-free formalism

Numerical applications presented in this work adopt a spin-free formulation of GVB-rCCD facilitated by the Unitary Group Approach (UGA) [41], as described in Ref. [32]. The SR ring approximation is not invariant to the various alternative treatments of spin during the derivation of equations. The situation is analogous in the MR case, spin-orbital and UGA parametrizations of GVB-rCCD being non-equivalent. The major findings of Sect. 2, however, hold for the UGA case as well, the only difference being that the second-order approximation of the dispersion energy is 5/4 times that of (12). In the following, we give a brief account of GVB-rCCD(UGA) used for obtaining the pilot results. The cluster operator is parametrized as

$$T = \frac{1}{2} \sum_{i,j,a,b} t_{ab}^{ij} \sum_{\sigma,\sigma'} a_{i\sigma j\sigma'}^{a\sigma b\sigma'} = \frac{1}{2} \sum_{i,j,a,b} t_{ab}^{ij} E_{ij}^{ab}, \tag{17}$$

with $t_{ab}^{ij} = t_{ba}^{ji}$. Indices i, j, k, l and a, b, c, d belong to core/active and active/virtual spatial orbitals, respectively. The energy formula reads:

$$\Delta E = \sum_{i,j,a,b} B_{ij}^{ab} t_{ab}^{ij} n_i n_j \bar{n}^a \bar{n}^b, \tag{18}$$

and the amplitude equation takes the form:

$$0 = B_{ab}^{ij} + 2 \sum_{k,c} \left(t_{ac}^{ik} A_{kb}^{cj} + A_{ak}^{ic} t_{cb}^{kj} \right) + 4 \sum_{k,c,l,d} t_{ac}^{ik} B_{kl}^{cd} t_{db}^{lj} n_k n_l \bar{n}^c \bar{n}^d, \tag{19}$$

where

$$B_{ij}^{ab} = \frac{1}{2} \mathcal{V}_{ij}^{ab},$$
$$A_{ib}^{aj} = \frac{1}{2} \left(\mathcal{F}_b^a \, \delta_i^j \, \bar{n}^a - \mathcal{F}_i^j \, \delta_b^a \, n_i + \mathcal{V}_{ib}^{aj} \, n_i \bar{n}^a \right).$$

The algebraic expressions of spin-free vertices are given in "Appendix 1".

There are two technical issues to address when solving (19). The first is the redundancy of excited states used for projection, which is presently handled based on the concept of frames [42, 43]. The associated numerical threshold for identifying zero eigenvalues of the overlap matrix is set to

$s_{\min} = 10^{-10}$. The second issue concerns the removal of certain kinds of excitations which could otherwise make the vertices and thus the amplitudes singular. To prevent this, an excitation selection scheme has been set up: excitation E_{ij}^{ab} is allowed in (17) only if

- (i) $n_i \bar{n}^a > 1/4$ for $i \neq a$ and $\mathcal{I} = \mathcal{A}$,
- (ii) $n_i \bar{n}^b > 1/4$ for $i \neq b$ and $\mathcal{I} = \mathcal{B}$,
- (iii) $n_j \bar{n}^a > 1/4$ for $j \neq a$ and $\mathcal{J} = \mathcal{A}$,
- (iv) $n_j \bar{n}^b > 1/4$ for $j \neq b$ and $\mathcal{J} = \mathcal{B}$,
- (v) $n_i > 1/2$ for $i = j$,
- (vi) $\bar{n}^a > 1/2$ for $a = b$,

calligraphic letters denoting geminal indices. All other excitations (including spectators, such as E_{ij}^{aj}) are allowed. The above constraints can be introduced in the results of Sect. 2 without any problem. Restricting the excitations this way does not violate size consistency.

GVB-rCCD(UGA) dispersion energy curves are presented for He_2 and Ne_2. The results are compared to the GVB-ERPA method of Pernal et al. [28, 29], and HF-CCSD(T) is used as benchmark. Calculations based on the GVB reference were performed by the Budapest version of the MUNGAUSS program package [44], and HF-CCSD(T) was calculated with the Gaussian 09 software [45]. Calculations were carried out using the Dunning aug-cc-pVDZ atomic basis set [46] (with five d-orbitals).

All calculations assume GVB natural orbitals, with geminals consisting of two orbitals, except for core geminals (having only one orbital).

In reporting the results, E_{disp} stands for the total energy of the supersystem minus total energies of the subsystems, computed according to the Boys–Bernardi scheme [47]. Total energy is calculated as the sum of the GVB energy and ΔE of (18).

Equilibrium atomic distances and the corresponding dispersion energies are given in Table 1, while Figs. 1 and 2 show the dispersion energy curves for He_2 and Ne_2, respectively. Just like HF, GVB cannot describe dispersion interactions, resulting in non-bonding energy curves. GVB-ERPA and GVB-rCCD(UGA) improve significantly on this situation, although the results are far from perfect. While GVB-ERPA underestimates the dispersion energy in both cases, GVB-rCCD(UGA) overestimates it, although to a somewhat lesser extent. A more significant difference shows up in the equilibrium atomic distances: GVB-ERPA overshoots by 0.4 bohr in each case, while GVB-rCCD(UGA) reproduces the benchmark CCSD(T) value to the digits displayed in Table 1.

Deficiencies of GVB-ERPA have been noted before in describing weak interaction, and electron-groups embedding has been suggested as a cure (GVB-EERPA) [30, 31].

It was also demonstrated that GVB-EERPA represents a significant improvement over GVB-ERPA in such situations. Comparison with GVB-ERPA is warranted here, since this unamended version represents the theory paralleling GVB-rCCD which is of prime interest in this study.

4 Conclusions

A recently proposed GVB-rCCD method built with dressed vertices (20) and (21) has been investigated concerning the calculation of dispersion interactions of noble gas dimers. An analytical inspection has revealed that the GVB-rCCD dispersion energy follows the correct $\sim 1/R^6$ asymptotic decay, and in the leading order of the energy, the dispersion coefficient can be expressed in terms uncoupled FDPs that involve a dressing taking into account the MR character of the reference function. Pilot numerical tests of full GVB-rCCD result in dispersion energies and equilibrium atomic distances in fairly good agreement with benchmark data.

Analysis of the $R \to \infty$ asymptotics of the full GVB-rCCD scheme is warranted as a continuation of this study since an expression of the form of (16) may arise with improved FDPs [2, 15], depending on the incorporation of exchange terms in
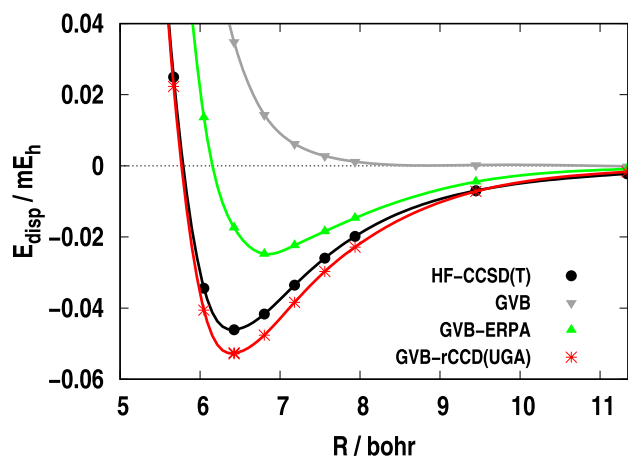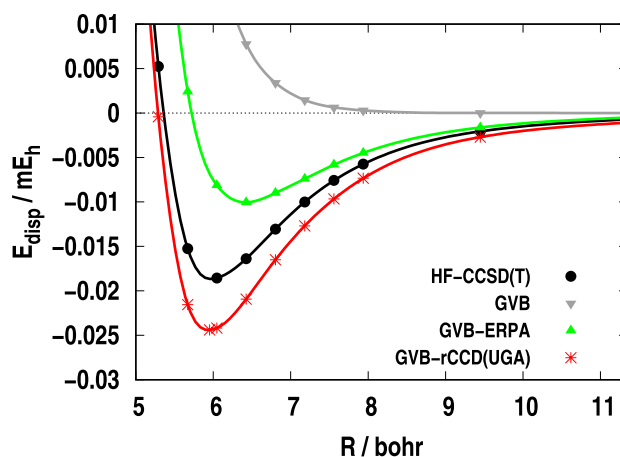

Fig. 1 Dispersion energy of He$_2$, calculated on the aug-cc-pVDZ basis set

the equations. Our current formulation is not favourable in this respect. Investigation in the line of GVB-rCCD variants yielding a C_6 expressed with coupled FDPs is deferred to a follow-up study.

Improving upon the correlation content of the equations, i.e. stepping beyond the ring approximation, is a further line of research for the future. This can be done by a systematic inclusion of a couple of types of non-ring diagrams, expressed with dressed vertices. Derivation and testing of these more involved MR-CC schemes shall be the subject of a forthcoming paper.

Availability of data and material Computational data behind the results reported are available upon request to the authors.

Code availability Budapest-MUNGAUSS is a custom code, and the Gaussian software is available commercially.

Compliance with ethical standards

Conflict of interest The authors declare that they have no conflict of interest.

Fig. 2 Dispersion energy of Ne$_2$, calculated on the aug-cc-pVDZ basis set

Table 1 Equilibrium atomic distances and interaction energies $E_{int} = E_{disp}(R_{min})$ for He$_2$ and Ne$_2$, calculated on the aug-cc-pVDZ basis set

	He$_2$		Ne$_2$	
	R_{min}/bohr	E_{int}/mE$_h$	R_{min}/bohr	E_{int}/mE$_h$
HF-CCSD(T)	6.0	− 0.0186	6.4	− 0.0461
GVB-ERPA	6.4	− 0.0101	6.8	− 0.0248
GVB-rCCD(UGA)	6.0	− 0.0244	6.4	− 0.0529

Appendix 1: Vertices appearing in the MR-rCCD equations

The bare vertices are $f_{p\sigma}^{q\sigma'} = f_q^p \delta_\sigma^{\sigma'}$ and $\tilde{v}_{p\sigma r\sigma''}^{q\sigma' s\sigma'''} = v_{pr}^{qs} \delta_\sigma^{\sigma'} \delta_{\sigma''}^{\sigma'''} - v_{rp}^{qs} \delta_{\sigma''}^{\sigma'} \delta_\sigma^{\sigma'''}$, with

$$f_p^q = h_p^q + \sum_r \bar{v}_{pr}^{qs} n_r,$$

$$h_p^q = \int d^3 r\, \phi_p^*(\boldsymbol{r}) \left(-\frac{1}{2}\nabla^2 - \sum_{\mathbb{A}} \frac{Z_{\mathbb{A}}}{|\boldsymbol{r} - \boldsymbol{R}_{\mathbb{A}}|} \right) \phi_q(\boldsymbol{r}),$$

$$v_{pr}^{qs} = \int d^3 r_1 \int d^3 r_2\, \phi_p^*(\boldsymbol{r}_1) \phi_r^*(\boldsymbol{r}_2) \frac{1}{|\boldsymbol{r}_1 - \boldsymbol{r}_2|} \phi_s(\boldsymbol{r}_2) \phi_q(\boldsymbol{r}_1),$$

$$\bar{v}_{pr}^{qs} = 2 v_{pr}^{qs} - v_{rp}^{qs}.$$

Indices p, q, r, s correspond to arbitrary spatial orbitals.

The spin-orbital dressed vertices read at the one-particle level:

$$\begin{aligned}
\zeta_U \zeta^X F_U^X &= \zeta_U \zeta^X f_U^X - \sum_{P,Q} f_P^Q\, \lambda_{QU}^{PX} \\
&\quad - \frac{1}{2} \sum_{P,Q,R} \left(\zeta^X \tilde{v}_{PR}^{XQ}\, \lambda_{UQ}^{PR} + \zeta_U \tilde{v}_{UQ}^{PR}\, \lambda_{PR}^{XQ} \right) \\
&\quad - \frac{1}{4} \sum_{P,Q,R,S} \tilde{v}_{PR}^{QS}\, \lambda_{QSU}^{PRX},
\end{aligned} \tag{20}$$

and at the two-particle level:

$$\begin{aligned}
\zeta_U \zeta^X \zeta_W \zeta^Y &V_{UW}^{XY} \\
&= \zeta_U \zeta^X \zeta_W \zeta^Y \tilde{v}_{UW}^{XY} \\
&\quad + \sum_P \left[\mathcal{A}^{XY}\left(\zeta^X f_P^X \lambda_{UW}^{PY} \right) + \mathcal{A}_{UW}\left(\zeta_U f_U^P \lambda_{PW}^{XY} \right) \right] \\
&\quad + \frac{1}{2} \sum_{P,Q} \left(\zeta^X \zeta^Y \tilde{v}_{PQ}^{XY} \lambda_{UW}^{PQ} + \zeta_U \zeta_W \tilde{v}_{UW}^{PQ} \lambda_{PQ}^{XY} \right) \\
&\quad - \sum_{P,Q} \mathcal{A}_{UW} \mathcal{A}^{XY}\left(\zeta_U \zeta^X \tilde{v}_{UP}^{XQ} \lambda_{WQ}^{YP} \right) \\
&\quad + \frac{1}{4} \sum_{P,Q,R,S} \tilde{v}_{PR}^{QS} \lambda_{UW}^{PR} \lambda_{QS}^{XY} + \sum_{P,Q,R,S} \tilde{v}_{PR}^{QS} \mathcal{A}_{UW}\left(\lambda_{QU}^{PX} \lambda_{SW}^{RY} \right) \\
&\quad - \frac{1}{2} \sum_{P,Q,R,S} \tilde{v}_{PR}^{QS} \left[\mathcal{A}^{XY}\left(\lambda_{QS}^{PX} \lambda_{UW}^{RY} \right) + \mathcal{A}_{UW}\left(\lambda_{QU}^{PR} \lambda_{SW}^{XY} \right) \right] \\
&\quad + \sum_{P,Q} f_P^Q \lambda_{UWQ}^{XYP} + \frac{1}{2} \sum_{P,Q,R} \left[\mathcal{A}^{XY}\left(\zeta^X \tilde{v}_{PR}^{QX} \lambda_{UWQ}^{RYP} \right) \right. \\
&\quad \left. + \mathcal{A}_{UW}\left(\zeta_U \tilde{v}_{UP}^{RQ} \lambda_{RWQ}^{XYP} \right) \right] + \frac{1}{4} \sum_{P,Q,R,S} \tilde{v}_{PR}^{QS} \lambda_{UWQS}^{XYPR}.
\end{aligned} \tag{21}$$

Indices P, Q, R, S correspond to arbitrary spin orbitals, and λ denotes the spin-orbital cumulants [35, 39]. In this paper, we distinguish between indices corresponding to core/active (I, J, K, L) and active/virtual (A, B, C, D) orbitals. Different dressed vertices belong to the different combination of indices, distinguished by the values ζ takes:

$$\zeta_U = \begin{cases} -n_U & \text{if} \quad U \in \{I, J, K, L\} \\ \bar{n}_U & \text{if} \quad U \in \{A, B, C, D\}. \end{cases} \tag{22}$$

The spin summation of (20) and (21) yields the spin-free dressed vertices:

$$\begin{aligned}
\zeta_u \zeta^x \mathcal{F}_u^x &= \zeta_u \zeta^x \sum_\sigma F_{u\sigma}^{x\sigma} \\
&= 2 \zeta_u \zeta^x f_u^x - \sum_{p,q} f_p^q \Lambda_{qu}^{px} \\
&\quad - \sum_{p,q,r} \left(\zeta^x v_{pr}^{xq} \Lambda_{uq}^{pr} + \zeta_u v_{uq}^{pr} \Lambda_{pr}^{xq} \right) - \frac{1}{2} \sum_{p,q,r,s} v_{pr}^{qs} \Lambda_{qsu}^{prx},
\end{aligned} \tag{23}$$

and

$$\begin{aligned}
\zeta_u \zeta^x \zeta_w & \zeta^y \mathcal{V}_{uw}^{xy} \\
&= \zeta_u \zeta^x \zeta_w \zeta^y \sum_{\sigma,\sigma'} V_{u\sigma w\sigma'}^{x\sigma y\sigma'} \\
&= 2 \zeta_u \zeta^x \zeta_w \zeta^y \bar{v}_{uw}^{xy} + \sum_p \left(\zeta^x f_p^x \Lambda_{uw}^{py} + \zeta_u f_u^p \Lambda_{pw}^{xy} + \zeta^y f_p^y \Lambda_{uw}^{xp} \right. \\
&\quad \left. + \zeta_w f_w^p \Lambda_{up}^{xy} \right) \\
&\quad + \sum_{p,q} \left(\zeta^x \zeta^y v_{pq}^{xy} \Lambda_{uw}^{pq} + \zeta_u \zeta_w v_{uw}^{pq} \Lambda_{pq}^{xy} - \zeta_w \zeta^y \bar{v}_{wp}^{yq} \Lambda_{uq}^{xp} \right. \\
&\quad \left. - \zeta_u \zeta^x \bar{v}_{up}^{xq} \Lambda_{wq}^{yp} \right) \\
&\quad + \sum_{p,q} \left[\zeta_w \zeta^x \left(v_{wp}^{qx} \Lambda_{uq}^{py} + v_{wp}^{xq} \Lambda_{uq}^{yp} \right) \right. \\
&\quad \left. + \zeta_u \zeta^y \left(v_{up}^{qy} \Lambda_{wq}^{px} + v_{up}^{yq} \Lambda_{wq}^{xp} \right) \right] \\
&\quad + \frac{1}{2} \sum_{p,q,r,s} \left[\bar{v}_{pr}^{qs} \Lambda_{uq}^{xp} \Lambda_{ws}^{yr} - v_{pr}^{qs} \left(\Lambda_{uw}^{py} \Lambda_{qs}^{xr} + \Lambda_{uw}^{xp} \Lambda_{qs}^{yr} + \Lambda_{us}^{pr} \Lambda_{qw}^{xy} \right. \right. \\
&\quad \left. \left. + \Lambda_{uq}^{xy} \Lambda_{ws}^{pr} + \Lambda_{uq}^{yp} \Lambda_{ws}^{xr} \right) \right] \\
&\quad + \frac{1}{6} \sum_{p,q,r,s} v_{pr}^{qs} \left[\Lambda_{uw}^{pr} \left(2\Lambda_{qs}^{xy} + \Lambda_{sq}^{xy} \right) + \Lambda_{us}^{yp} \left(2\Lambda_{wq}^{xr} + \Lambda_{wq}^{rx} \right) \right. \\
&\quad \left. + \Lambda_{us}^{py} \left(2\Lambda_{wq}^{rx} + \Lambda_{wq}^{xr} \right) \right] \\
&\quad + \sum_{p,q} f_p^q \Lambda_{uwq}^{xyp} + \sum_{p,q,r} \left(\zeta^x v_{pr}^{qx} \Lambda_{uwq}^{ryp} + \zeta_u v_{up}^{rq} \Lambda_{rwq}^{xyp} \right. \\
&\quad \left. + \zeta^y v_{pr}^{qy} \Lambda_{uwq}^{xrp} + \zeta_w v_{wp}^{rq} \Lambda_{urq}^{xyp} \right) \\
&\quad + \frac{1}{2} \sum_{p,q,r,s} v_{pr}^{qs} \Lambda_{uwqs}^{xypr}.
\end{aligned} \tag{24}$$

Function ζ in the above is the analogue of (22), with all orbital indices in lower case. Spin-free cumulants are denoted by Λ; see "Appendix 2" for the corresponding formulae.

In order to make the arguments of "Appendix 3" easier to follow, we give the explicit formulae for $\mathcal{F}$ with both indices being either core/active or active/virtual type:

$$
\begin{aligned}
n_i n^j \mathcal{F}_i^j = {} & 2 n_i n^j f_i^j - \sum_{p,q} f_p^q \Lambda_{qi}^{pj} + \sum_{p,q,r} \left(n^j v_{pr}^{jq} \Lambda_{iq}^{pr} + n_i v_{iq}^{pr} \Lambda_{pr}^{jq} \right) \\
& - \frac{1}{2} \sum_{p,q,r,s} v_{pr}^{qs} \Lambda_{qsi}^{prj},
\end{aligned}
\tag{25}
$$

$$
\begin{aligned}
\bar{n}_b \bar{n}^a \mathcal{F}_b^a = {} & 2 \bar{n}_b \bar{n}^a f_b^a - \sum_{p,q} f_p^q \Lambda_{qb}^{pa} - \sum_{p,q,r} \left(\bar{n}^a v_{pr}^{aq} \Lambda_{bq}^{pr} + \bar{n}_b v_{bq}^{pr} \Lambda_{pr}^{aq} \right) \\
& - \frac{1}{2} \sum_{p,q,r,s} v_{pr}^{qs} \Lambda_{qsb}^{pra}.
\end{aligned}
\tag{26}
$$

For singlet systems, the relation between spin-orbital tensors invariant under spin rotations and their spin-free counterparts was established by Shamasundar (originally discussed in the context of density matrices and cumulants) [40, 48]. The same kind of formulae is applied to the dressed vertices as well:

$$
F_{i\alpha}^{a\alpha} = \frac{1}{2} \mathcal{F}_i^a,
\tag{27}
$$

and

$$
V_{i\alpha j\alpha}^{a\alpha b\alpha} = \frac{1}{6}\left(\mathcal{V}_{ij}^{ab} - \mathcal{V}_{ji}^{ab} \right), \quad V_{i\alpha j\beta}^{a\alpha b\beta} = \frac{1}{6}\left(2\mathcal{V}_{ij}^{ab} + \mathcal{V}_{ji}^{ab} \right).
\tag{28}
$$

The vertices are invariant to spin-flip, and they vanish in all spin non-conserving cases.

Appendix 2: The structure of spin-free GVB cumulants

The calculation of dressed vertices (23)–(26) requires cumulants up to rank four. Computation and storage of such a cumulant (having eight indices running through all active orbitals) would be computationally too demanding, for example, for a CAS-type reference function. Strongly orthogonal geminal functions, on the other hand, offer a relatively simple and economic way to generate cumulants. Strong orthogonality implies the vanishing of all cumulant elements with indices belonging to different geminals [39]: for GVB, this condition renders the maximal number of nonzero elements in Λ_K to only $N2^{2K-1}$. Because of strong orthogonality, cumulant terms in (23)–(26) are actually less

expensive to calculate than SR terms, leading to GVB-rCCD exhibiting the same computational scaling as SR-rCCD.

Here, we give the spin-free expressions of GVB cumulants up to rank three:

$$
\begin{aligned}
\Lambda_q^p &= 2\delta_q^p n_p, \\
\Lambda_{qs}^{pr} &= 2\delta_Q^P c^p c_q \delta^{pr} \delta_{qs} - \delta^{PR}\left(\Lambda_q^p \Lambda_s^r - \frac{1}{2} \Lambda_s^p \Lambda_q^r \right),
\end{aligned}
\tag{29}
$$

$$
\begin{aligned}
\Lambda_{qsu}^{prt} = {} & -\delta^{PR}\delta^{RT}\delta^{TP}\Big(\Lambda_q^p \Lambda_s^r \Lambda_u^t - \frac{1}{2} \Lambda_q^p \Lambda_u^r \Lambda_s^t + \frac{1}{4} \Lambda_u^p \Lambda_q^r \Lambda_s^t \\
& - \frac{1}{2} \Lambda_u^p \Lambda_s^r \Lambda_q^t + \frac{1}{4} \Lambda_s^p \Lambda_u^r \Lambda_q^t - \frac{1}{2} \Lambda_s^p \Lambda_q^r \Lambda_u^t \Big) - \\
& - \delta^{PR}\left(\Lambda_q^p \Lambda_{su}^{rt} - \frac{1}{2} \Lambda_s^p \Lambda_{qu}^{rt} - \frac{1}{2} \Lambda_u^p \Lambda_{sq}^{rt} \right) \\
& - \delta^{RT}\left(\Lambda_s^r \Lambda_{uq}^{tp} - \frac{1}{2} \Lambda_u^r \Lambda_{sq}^{tp} - \frac{1}{2} \Lambda_q^r \Lambda_{us}^{tp} \right) \\
& - \delta^{TP}\left(\Lambda_u^t \Lambda_{qs}^{pr} - \frac{1}{2} \Lambda_q^t \Lambda_{us}^{pr} - \frac{1}{2} \Lambda_s^t \Lambda_{qu}^{pr} \right).
\end{aligned}
\tag{30}
$$

The expression of the rank four cumulant (Λ_4) is too lengthy to be presented; it can be, however, easily manipulated with the aid of symbolic algebra codes.

Appendix 3: On the positivity of ϵ_i^a

In Sect. 2, when expressing C_6 in terms of FDP-like quantities (see (16)) we assumed the positivity of ϵ_i^a (defined in (5)), a statement supported by numerical results for GVB, tested in various (e.g. bond breaking) scenarios. While we cannot prove this statement in an exact way, we can provide some formal rationalization based on certain reasonable assumptions concerning the diagonal elements of the GVB Fockian: f_p^p is assumed to be negative if orbital p is strongly occupied ($n_p \lesssim 1$) and positive (or negative with a very small absolute value) if p is weakly occupied ($n_p \gtrsim 0$). Furthermore, GVB geminals consist of two orbitals, here denoted as $i, i' \in \mathcal{I}$ and $a, a' \in \mathcal{A}$, so that $n_i + n_{i'} = n_a + n_{a'} = 1$. With the help of (27), ϵ_i^a of (5) can be written equivalently as

$$
\epsilon_i^a = \frac{1}{2}\left(\bar{n}^a \mathcal{F}_a^a - n_i \mathcal{F}_i^i \right).
$$

Using the explicit form of the GVB Λ_2 and Λ_3 given by (29) and (30), one can express (25) and (26) as

$$
\begin{aligned}
\frac{1}{2} n_i \mathcal{F}_i^i = {} & (2n_i - 1) f_i^i + 2\bar{n}_i f_{i'}^{i'} + 2n_i \bar{n}_i v_{ii}^{ii} \\
& - 2\sqrt{n_i \bar{n}_i}\, v_{i'i'}^{ii} - 2n_i \bar{n}_i \bar{v}_{ii'}^{ii'} - \bar{n}_i(2n_i - 1)(\bar{v}_{ii'}^{ii'} - v_{i'i'}^{i'i'}), \\
\frac{1}{2} \bar{n}^a \mathcal{F}_a^a = {} & -(2n^a - 1) f_a^a + 2n_a f_{a'}^{a'} - 2n_a \bar{n}_a v_{aa}^{aa} \\
& + 2\sqrt{n_a \bar{n}_a}\, v_{a'a'}^{aa} + 2n_a \bar{n}_a \bar{v}_{aa'}^{aa'} - n_a(2n_a - 1)(\bar{v}_{aa'}^{aa'} - v_{a'a'}^{a'a'}).
\end{aligned}
$$

In the above, we made use of the fact that the coefficients of orbitals i and i' have opposite signs (the same applying to a and a'). Real orbitals are assumed.

We shall analyse these expressions in two limiting cases: the HF-like case (one orbital in the geminal is strongly occupied, and the other is weakly occupied) and the case of the dissociating geminal (both orbitals in the geminal having the same occupation). We have:

$$n_i \approx 1 \;\rightarrow\; \frac{1}{2}n_i\mathcal{F}_i^i \approx f_i^i, \tag{31}$$

$$n_i \approx 0 \;\rightarrow\; \frac{1}{2}n_i\mathcal{F}_i^i \approx -f_i^i + 2f_{i'}^i - \left(v_{i'i'}^{i'i'} + v_{i'i'}^{ii} - 2v_{ii'}^{ii'}\right), \tag{32}$$

$$
\begin{aligned}
n_i \approx \frac{1}{2} \;\rightarrow\; \frac{1}{2}n_i\mathcal{F}_i^i &\approx f_{i'}^i \\
&+ \frac{1}{2}\left(v_{ii}^{ii} - v_{i'i'}^{ii} - 2v_{ii'}^{ii'}\right) \approx f_i^i - \frac{1}{2}\left(v_{ii}^{ii} + v_{i'i'}^{ii}\right),
\end{aligned} \tag{33}
$$

$$\bar{n}^a \approx 1 \;\rightarrow\; \frac{1}{2}\bar{n}^a\mathcal{F}_a^a \approx f_a^a, \tag{34}$$

$$\bar{n}^a \approx 0 \;\rightarrow\; \frac{1}{2}\bar{n}^a\mathcal{F}_a^a \approx -f_a^a + 2f_{a'}^a + \left(v_{a'a'}^{a'a'} + v_{a'a'}^{aa} - 2v_{aa'}^{aa'}\right), \tag{35}$$

$$
\begin{aligned}
\bar{n}^a \approx \frac{1}{2} \;\rightarrow\; \frac{1}{2}\bar{n}^a\mathcal{F}_a^a &\approx f_{a'}^a \\
&- \frac{1}{2}\left(v_{aa}^{aa} - v_{a'a'}^{aa} - 2v_{aa'}^{aa'}\right) \approx f_a^a + \frac{1}{2}\left(v_{aa}^{aa} + v_{a'a'}^{aa}\right).
\end{aligned} \tag{36}
$$

We used the fact that in the dissociating regime $f_i^i \approx f_{i'}^i$ and $v_{ii}^{ii} \approx v_{i'i'}^{i'i'} \approx v_{ii'}^{ii'}$ (and similar relations for a). Note that in the weakly interacting case considered in this paper, geminals are localized on subsystems. A dissociating geminal is assumed to be part of the subsystem, e.g. a molecule with stretched geometry. In this paper, the case $n_i \approx 1/2$ does not appear, all subsystems being closed-shell atoms.

All two-electron integrals appearing in (31)–(36) are positive. The two-electron contribution is small compared to the Fockian part around equilibrium geometry, while it is the other way around in the dissociating regime. Based on these equations and our initial assumption concerning the sign of f_p^p, one can argue the positivity of ϵ_i^a. In, for example, (32), $2f_{i'}^i$ is expected to give the (large negative) dominant contribution. The positivity of the dominant contribution in (35) can be argued similarly, leading to the positivity of ϵ_i^a, despite ϕ_i and ϕ_a being weakly and strongly occupied, respectively. As a further example, let us assume a dissociating geminal with $\mathcal{I} = \mathcal{A}, i \neq a$ and $n_i \approx n_a \approx 1/2$. Then $i' = a$ and $a' = i$. Using (33) and (36), ϵ_i^a reads:

$$\epsilon_i^a \approx v_{ii}^{ii} + v_{ii}^{aa} \geq 0.$$

References

1. Kaplan IG (2006) Intermolecular interactions: physical picture, computational methods and model potentials. Wiley, Hoboken
2. Szabo A, Oslund NS (1977) J Chem Phys 67:4351
3. Langhoff PW, Karplus M, Hurst RP (1966) J Chem Phys 44:505
4. Jeziorski B, Moszynski R, Szalewicz K (1994) Chem Rev 94:1887
5. Chałasiński G, Szcześniak MM (1987) Mol Phys 63:205
6. Moszynski R, Jeziorski B, Szalewicz K (1993) Int J Quantum Chem 45:409
7. Szabo A, Oslund NS (1977) Int J Quantum Chem 11:389
8. Bartlett RJ, Musiał M (2007) Rev Mod Phys 79:291
9. Shavitt I, Bartlett RJ (2009) Many-body methods in chemistry and physics. Cambridge University Press, Cambridge
10. Raghavachari K, Trucks GW, Pople JA, Head-Gordon M (1989) Chem Phys Lett 157:479
11. Čížek J (1966) J Chem Phys 45:4256
12. Scuseria GE, Henderson TM, Sorensen DC (2008) J Chem Phys 129:231101
13. Jansen G, Liu R-F, Ángyán JG (2010) J Chem Phys 133:154106
14. Ren X, Rinke P, Joas C, Scheffler M (2012) J Mater Sci 47:7447
15. Dobson JF (1994) Quasi-local-density approximation for a van der Waals energy functional. In: Das MP (ed) Topics in condensed matter physics. Nova, Hauppauge, p 121
16. Dobson JF, McLennan K, Rubio A, Wang J, Gould T, Le HM, Dinte BP (2001) Aust J Chem 54:513
17. Furche F (2008) J Chem Phys 129:114105
18. Grüneis A, Marsman M, Harl J, Schimka L, Kresse G (2009) J Chem Phys 131:154115
19. Paier J, Janesko BG, Henderson TM, Scuseria GE, Grüneis A, Kresse G (2010) J Chem Phys 132:094103
20. Ren X, Rinke P, Scuseria GE, Scheffler M (2013) Phys Rev B 88:035120
21. Hehn A-S, Tew DP, Klopper W (2015) J Chem Phys 142:194106
22. Toulouse J, Zhu W, Ángyán JG, Savin A (2010) Phys Rev A 82:032502
23. Toulouse J, Zhu W, Savin A, Jansen G, Ángyán JG (2011) J Chem Phys 135:084119
24. Surján PR (1999) An introduction to the theory of geminals. In: Surján PR (ed) Topics in current chemistry 203: correlation and localization. Springer, Berlin, p 63
25. Arai T (1960) J Chem Phys 33:95
26. Goddard WA, Dunning TH, Hunt WJ, Hay PJ (1973) Acc Chem Res 6(11):368
27. Zoboki T, Szabados Á, Surján PR (2013) J Chem Theory Comput 9:2602
28. Pernal K (2014) J Chem Theory Comput 10:4332
29. Pastorczak E, Pernal K (2015) Phys Chem Chem Phys 17:8622
30. Pastorczak E, Shen J, Hapka M, Piecuch P, Pernal K (2017) J Chem Theory Comput 13:5404
31. Pastorczak E, Pernal K (2018) Theor Chem Acc 137:172
32. Margócsy Á, Szabados Á (2020) J Chem Phys 152:204114
33. Mahapatra U, Datta B, Bandyopadhyay B, Mukherjee D (1998) Adv Quantum Chem 30:163
34. Szabados Á, Margócsy Á (2017) Mol Phys 115:2731
35. Mukherjee D, Kutzelnigg W (1997) J Chem Phys 107:432
36. Lindgren I (1978) Int J Quantum Chem 14:33
37. Hanauer M, Köhn A (2012) Chem Phys 401:50
38. Fukuda N, Iwamoto F, Sawada K (1964) Phys Rev A 135:A932
39. Mukherjee D, Kutzelnigg W (1998) J Chem Phys 110:2800
40. Kutzelnigg W, Shamasundar KR, Mukherjee D (2010) Mol Phys 108:433
41. Paldus J, Boyle MJ (1980) Phys Scr 21:295
42. Morgenshtern VI, Bölcskei H (2012) A short course on frame theory. In: Serpedin TCE, Rajan D (eds) Mathematical foundations

for signal processing, communications, and networking. CRC, Boca Raton, pp 737–789

43. Casazza PG, Kutyniok G, Philipp F (2012) Introduction to finite frame theory. In: Casazza PG, Kutyniok G (eds) Finite frames: theory and applications. Birkhäuser, Basel, pp 1–54

44. Surján PR (2002) Program BP-MUNGAUSS. Department of Theoretical Chemistry, Eötvös University, Budapest

45. Frisch MJ, Trucks GW, Schlegel HB, Scuseria GE, Robb MA, Cheeseman JR, Scalmani G, Barone V, Mennucci B, Petersson GA, Nakatsuji H, Caricato M, Li X, Hratchian HP, Izmaylov AF, Bloino J, Zheng G, Sonnenberg JL, Hada M, Ehara M, Toyota K, Fukuda R, Hasegawa J, Ishida M, Nakajima T, Honda Y, Kitao O, Nakai H, Vreven T, Montgomery JA Jr, Peralta JE, Ogliaro F, Bearpark M, Heyd JJ, Brothers E, Kudin KN, Staroverov VN, Keith T, Kobayashi R, Normand J, Raghavachari K, Rendell A, Burant JC, Iyengar SS, Tomasi J, Cossi M, Rega N, Millam JM, Klene M, Knox JE, Cross JB, Bakken V, Adamo C, Jaramillo J, Gomperts R, Stratmann RE, Yazyev O, Austin AJ, Cammi R, Pomelli C, Ochterski JW, Martin RL, Morokuma K, Zakrzewski VG, Voth GA, Salvador P, Dannenberg JJ, Dapprich S, Daniels AD, Farkas O, Foresman JB, Ortiz JV, Cioslowski J, Fox DJ (2010) Gaussian 09, Revision B.01. Gaussian, Inc., Wallingford CT

46. Dunning TH (1989) J Chem Phys 90:1007

47. Boys SF, Bernardi F (1970) Mol Phys 19(4):553

48. Shamasundar KR (2009) J Chem Phys 131:174109